Inorg. Chem. **2009**, *48*, 2664−2669

Conjugation of Selenophene with Bipyridine for a High Molar Extinction Coefficient Sensitizer in Dye-Sensitized Solar Cells

Feifei Gao,[†] Yueming Cheng,[†] Qingjiang Yu,[†] Shi Liu,[†,‡] Dong Shi,[†] Yunhui Li,[‡] and Peng Wang*[,†]

State Key Laboratory of Polymer Physics and Chemistry, Changchun Institute of Applied Chemistry, Chinese Academy of Sciences, Changchun 130022, China, and School of Chemistry and Environmental Engineering, Changchun University of Science and Technology, Changchun 130022, China

Received November 29, 2008

A high molar extinction coefficient heteroleptic polypyridyl ruthenium sensitizer, featuring a conjugated electron-rich selenophene unit in its ancillary ligand, has been synthesized and demonstrated as an efficient sensitizer in dye-sensitized solar cells. A nanocrystalline titania film stained with this sensitizer shows improved optical absorptivity, which is highly desirable for dye-sensitized solar cells with a thin photoactive layer. With preliminary testing, this sensitizer has already achieved a high efficiency of 10.6% measured under the air mass 1.5 global conditions.

Introduction

Low-cost excitonic solar cells[1] with organic optoelectronic materials as active components are receiving surging academic and industrial attention as potential candidates for the future photovoltaic market. In the family of organic photovoltaic devices, the mesoscopic dye-sensitized solar cell (DSC)[2] has achieved a respectable high efficiency and remarkable stability under prolonged thermal and light-soaking dual stress. It is fair to note that so far over 11% efficient DSCs can only be made with three polypyridyl ruthenium sensitizers[3] in combination with toxic and volatile acetonitrile-based electrolytes, while impressive device efficiencies have been reached with some other metal complexes[4] and metal-free dyes.[5] In further efforts to substitute these impractical electrolytes with nonvolatile or even solvent-free electrolytes, it is noted that with a low-fluidity electrolyte the charge collection yield becomes low due to the shortened electron diffusion length. Enhancing the optical absorptivity of a stained mesoporous film can counter this effect. Thus, a strategy of extending the conjugation of $Ru(dcbpy)(L)(NCS)_2$ (where dcbpy is 4,4′-dicarboxylic acid-2,2′-bipyridine and L is the ancillary ligand) photosensitizers has been actively explored to target this issue.[6]

In this context, the C101 dye with a 4,4′-bis(5-hexylthiophen-2-yl)-2,2′-bipyridine ligand has set a new DSC efficiency record of 11.3−11.5%,[7] becoming the first sensitizer triumphing over the well-known N3 dye reported 15 years ago. We have further noted that, in comparison with its analogue with a 4,4′-bis(5-hexylfuran-2-yl)-2,2′-bipyridine ligand, the C101 dye features a higher molar extinction coefficient by using low-electronegative sulfur in place of oxygen.[3c] It is also noted that, in contrast to poly(3-hexyl-

* To whom correspondence should be addressed. E-mail: peng.wang@ciac.jl.cn.
† Chinese Academy of Sciences.
‡ Changchun University of Science and Technology.

(1) (a) Gregg, B. A. *J. Phys. Chem. B* **2003**, *107*, 4688. (b) Gregg, B. A.; Hanna, M. C. *J. Appl. Phys.* **2003**, *93*, 3605. (c) Gregg, B. A.; Scott, B.; Gledhill, S. E. *J. Mater. Res.* **2005**, *20*, 3167. (d) For a special issue on organic-based photovoltaics, see: *MRS Bull.* **2005**, *30*, 10−53.
(2) (a) O'Regan, B.; Grätzel, M. *Nature* **1991**, *353*, 737. (b) Grätzel, M. *Nature* **2001**, *414*, 338. (c) Grätzel, M. *Inorg. Chem.* **2005**, *44*, 6841.
(3) (a) Nazeeruddin, M. K.; De Angelis, F.; Fantacci, S.; Selloni, A.; Viscardi, G.; Liska, P.; Ito, S.; Takeru, B.; Grätzel, M. *J. Am. Chem. Soc.* **2005**, *127*, 16835. (b) Chiba, Y.; Islam, A.; Watanabe, Y.; Komiya, R.; Koide, N.; Han, L. *Jpn. J. Appl. Phys., Part 2* **2006**, *45*, L638. (c) Gao, F.; Wang, Y.; Shi, D.; Zhang, J.; Wang, M.; Jing, X.; Humphry-Baker, R.; Wang, P.; Zakeeruddin, S. M.; Grätzel, M. *J. Am. Chem. Soc.* **2008**, *130*, 10720.
(4) (a) Ferrere, S.; Gregg, B. A. *J. Am. Chem. Soc.* **1998**, *120*, 843. (b) Sauvé, G.; Cass, M. E.; Doig, S. J.; Lauermann, I.; Pomykal, K.; Lewis, N. S. *J. Phys. Chem. B* **2000**, *104*, 3488. (c) Asbury, J. B.; Hao, E.; Wang, Y.; Lian, T. *J. Phys. Chem. B* **2000**, *104*, 11957. (d) Islam, A.; Sugihara, H.; Hara, K.; Singh, L. P.; Katoh, R.; Yanagida, M.; Takahashi, Y.; Murata, S.; Arakawa, H. *Inorg. Chem.* **2001**, *40*, 5371. (e) Geary, E. A. M.; Yellowlees, L. J.; Jack, L. A.; Oswald, L. D. H.; Parsons, S.; Hirata, N.; Durrant, J. R.; Robertson, N. *Inorg. Chem.* **2005**, *44*, 242. (f) Altobello, S.; Argazzi, R.; Caramori, S.; Contado, C.; Da Fré, S.; Rubino, P.; Choné, C.; Larramona, G.; Bignozzi, C. A. *J. Am. Chem. Soc.* **2005**, *127*, 15342. (g) Bessho, T.; Constable, E. C.; Grätzel, M.; Redondo, A. H.; Housecroft, C. E.; Kylberg, W.; Nazeeruddin, M. K.; Neuburger, M.; Schaffner, S. *Chem. Commun.* **2008**, 3717.
(5) Ito, S.; Miura, H.; Uchida, S.; Takata, M.; Sumioka, K.; Liska, P.; Comte, P.; Péchy, P.; Grätzel, M. *Chem. Commun.* **2008**, 5194, and references therein.

10.1021/ic802289e CCC: $40.75
Published on Web 01/30/2009

Scheme 1. Synthetic Route of the C105 Dye[a]

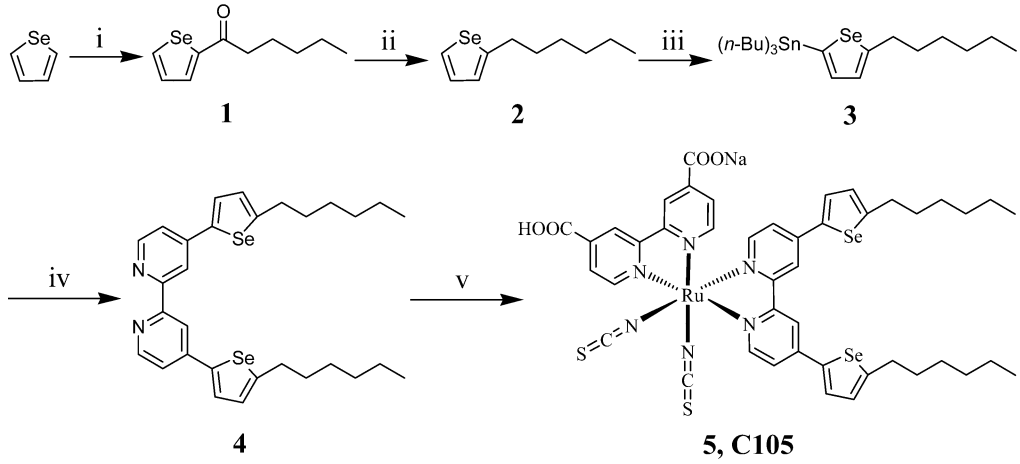

[a] (i) Hexanoyl chloride, $AlCl_3$, 0 °C; (ii) $LiAlH_4$, $AlCl_3$, r.t.; (iii) *n*-butyllithium, −78 °C, Bu_3SnCl, rt; (iv) 4,4′-dibromo-2,2′-bipyridine, $Pd(PPh_3)_2Cl_2$, toluene, reflux; (v) dichloro(*p*-cymene)ruthenium(II) dimmer, 4,4′-dicarboxylic acid-2,2′-bipyridine, NH_4NCS.

thiophene), poly(3-hexylselenophene) has a lower bandgap and broader photocurrent response.[8] Keeping these in mind, we have conjugated the selenophene unit with the bipyridyl ligand to construct a high molar extinction coefficient heteroleptic ruthenium sensitizer coded C105 and shown in Scheme 1. Through a series of parallel experiments, we have found that this new dye is very applicable to the production of efficient solar cells with very thin photoactive layers, in contrast to its counterpart, the standard amphiphilic Z907 dye. With preliminary testing, we have already fabricated a 10.6% efficiency solar cell measured under the air mass 1.5 global (AM1.5G) conditions.

Experimental Section

Materials. All solvents and reagents, unless otherwise stated, were of puriss quality and used as received. Selenophene, *n*-butyllithium, $[RuCl_2(p\text{-cymene})]_2$, and tetra-*n*-butylammonium hexafluorophosphate were purchased from Aldrich. Guanidinium thiocyanate (GNCS), 3α,7α-dihyroxy-5β-cholic acid (cheno), and *tert*-butylpyridine were purchased from Fluka. Sephadex LH-20 was obtained from Pharmacia. The solvent-free synthesis of 1,3-dimethylimidazolium iodide (DMII) was described in our previous paper.[9] 4,4′-Dibromo-2,2′-bipyridine[10] and *N*-butylbenzimidazole[11] were prepared according to the literature methods.

Synthesis of 1-(Selenophen-2-yl)-hexan-1-one (1). To a stirred solution of selenophene (1.00 g, 7.63 mmol) in anhydrous CH_2Cl_2 (30 mL) was added hexanoyl chloride (1.05 g, 7.83 mmol). The mixture was stirred for 30 min at room temperature, then cooled to 0 °C, and $AlCl_3$ (1.32 g, 9.90 mmol) was added portion-wise. The mixture was stirred for 2 h at that temperature. The reaction was quenched by the addition of water. The mixture was extracted with CH_2Cl_2. The organic layer was washed with water and dried over Na_2SO_4. After removing the solvent, the crude product was purified by column chromatography (ethyl acetate/petroleum ether, 1:10) on silica gel to afford a yellowish liquid (1.01 g, 60% yield). ^{1}H NMR (400 MHz, DMSO, δ_H): 8.61 (d, 1H, 3-***H*** of selenophene), 8.15 (d, 1H, 5-***H*** of selenophene), 7.48 (t, 1H, 4-***H*** of selenophene), 2.94 (t, 2H, $COCH_2$), 1.62−1.59 (m, 2H, $COCH_2CH_2$), 1.30−1.29 (m, 4H, $(CH_2)_2CH_3$), 0.86 (t, 3H, CH_3). MS (ESI) *m*/*z* calcd. for ($C_{10}H_{14}OSe$): 230.02. Found: 229.87.

Synthesis of 2-Hexylselenophene (2). $LiAlH_4$ (1.12 g, 29.6 mmol) and $AlCl_3$ (1.65 g, 12.35 mmol) were separatedly added to cold anhydrous ether (40 mL) slowly, and the resulting suspended solutions were carefully mixed. To this mixture was added 1-selenophen-2-yl-hexan-1-one (0.9 g, 3.94 mmol) in dry ether (10 mL) at 0 °C. The mixture was warmed to room temperature and then stirred for 3 h. The reaction was quenched by the careful addition of water. The gray precipitate was filtered off and washed with ether. The combined filtrate was extracted, washed with water, and dried over Na_2SO_4. After rotary evaporation of the solvent, the crude product was purified with column chromatography (ethyl acetate/petroleum ether, 1:10) on silica gel to afford a light yellow liquid (0.65 g, 76.5% yield). ^{1}H NMR (400 MHz, DMSO, δ_H): 7.91 (d, 1H, 5-***H*** of selenophene), 7.11 (q, 1H, 4-***H*** of selenophene), 6.97 (d, 1H, 3-***H*** of selenophene), 2.84 (t, 2H, $CH_2(CH_2)_4CH_3$), 1.61−1.58 (m, 2H, $CH_2(CH_2)_3CH_3$), 1.34−1.25 (m, 6H, $(CH_2)_3CH_3$), 0.86 (t, 3H, CH_3). MS (ESI) *m*/*z* calcd for ($C_{10}H_{16}Se$): 216.04. Found: 216.23.

(6) For the conceptual work, see: (a) Wang, P.; Zakeeruddin, S. M.; Moser, J.-E.; Humphry-Baker, R.; Comte, P.; Aranyos, V.; Hagfeldt, A.; Nazeeruddin, M. K.; Grätzel, M. *Adv. Mater.* **2004**, *16*, 1806. For other representative work, see: (b) Jiang, K.-J.; Masaki, N.; Xia, J.-B.; Noda, S.; Yanagida, S. *Chem. Commun.* **2006**, 2460. (c) Chen, C.-Y.; Wu, S.-J.; Wu, C.-G.; Chen, J.-G.; Ho, K.-C. *Angew. Chem., Int. Ed.* **2006**, *45*, 5822. (d) Karthikeyan, C. S.; Wietasch, H.; Thelakkat, M. *Adv. Mater.* **2007**, *19*, 1091. (e) Chen, C.-Y.; Wu, S.-J.; Li, J.-Y.; Wu, C.-G.; Chen, J.-G.; Ho, K.-C. *Adv. Mater.* **2007**, *19*, 3888. (f) Gao, F.; Wang, Y.; Zhang, J.; Shi, D.; Wang, M.; Humphry-Baker, R.; Wang, P.; Zakeeruddin, S. M.; Grätzel, M. *Chem. Commun.* **2008**, 2577. (g) Lee, C.; Yum, J.-H.; Choi, H.; Kang, S. O.; Ko, J.; Humphry-Baker, R.; Grätzel, M.; Nazeeruddin, M. K. *Inorg. Chem.* **2008**, *47*, 2267. (h) Chen, C.-Y.; Chen, J.-G.; Wu, S.-J.; Li, J.-Y.; Wu, C.-G.; Ho, K.-C. *Angew. Chem., Int. Ed.* **2008**, *47*, 7342. (i) Mater, F.; Ghaddar, T. H.; Walley, K.; Dos Santo, T.; Durrant, J. R.; O'Regan, B. *J. Mater. Chem.* **2008**, *18*, 4246.

(7) Thampi, K. R.; Bessho, T.; Gao, F.; Zakeeruddin, S. M.; Wang, P.; Grätzel, M. *23rd European Photovoltaic Solar Energy Conference and Exhibition*, Valencia, Spain, Sept. 1−4, 2008.

(8) (a) Heeney, M.; Zhang, W.; Crouch, D. J.; Chabinyc, M. L.; Gordeyev, S.; Hamilton, R.; Higgins, S. J.; McCulloch, I.; Skabara, P. J.; Sparrowe, D.; Tierney, S. *Chem. Commun.* **2007**, 5061. (b) Ballantyne, A. M.; Chen, L.; Nelson, J.; Bradley, D. D. C.; Astuti, Y.; Maurano, A.; Shuttle, C. G.; Durrant, J. R.; Duffy, W.; McCulloch, I. *Adv. Mater.* **2007**, *19*, 4544.

(9) Cao, Y.; Zhang, J.; Bai, Y.; Li, R.; Zakeeruddin, S. M.; Grätzel, M.; Wang, P. *J. Phys. Chem. C* **2008**, *112*, 13775.

(10) (a) Maerker, G.; Case, F. H. *J. Am. Chem. Soc.* **1958**, *80*, 2745. (b) Wenkert, D.; Woodward, R. B. *J. Org. Chem.* **1983**, *48*, 283.

(11) Pilarski, B. *Liebigs Ann. Chem.* **1983**, 1078.

Synthesis of 4,4′-Bis(5-hexylselenophen-2-yl)-2,2′-bipyridine (4). *n*-Butyllithium (2.27 mL, 1.6 M in hexane, 3.63 mmol) was added dropwise to a solution of 2-hexylselenophene (0.65 g, 3.02 mmol) in anhydrous THF at −78 °C under Ar. The mixture was stirred at this temperature for 1.5 h; tributylstannyl chloride was added (1.28 g, 3.93 mmol). After stirring for 6 h at room temperature, the reaction was terminated by adding water. The mixture was extracted with CH_2Cl_2 and dried over Na_2SO_4. After the removal of the solvent, crude 2-hexyl-5-tributylstannylselenophene (**3**) was mixed with 4,4′-dibromo-2,2′-bipyridine (0.32 g, 1.00 mmol) in 100 mL of toluene. The catalyst $Pd(PPh_3)_2Cl_2$ (0.039 g, 0.05 mmol) was added to the solution, and the mixture was refluxed under Ar overnight. After the rotary evaporation of toluene, the resulting solid was purified by column chromatography on silica gel using 1:10 CH_3OH/CHCl as an eluent to afford the target compound (0.468 g, 80% yield) as an ivory white solid. ^{1}H NMR (400 MHz, $CDCl_3$, δ_H): 8.63 (d, 4H, 3,3′,6,6′-***H*** of bipyridine), 7.71 (br, 2H, 5,5′-***H*** of bipyridine), 7.42 (br, 2H, 4-***H*** of selenophene), 7.01 (br, 2H, 3-***H*** of selenophene), 2.92 (t, 4H, 2 × C***H***$_2$(CH$_2$)$_4$CH$_3$), 1.74−1.69 (m, 4H, 2 × C***H***$_2$(CH$_2$)$_3$CH$_3$), 1.56−1.33 (m, 4H, 2 × C***H***$_2$(CH$_2$)$_2$CH$_3$), 1.33−1.32 (m, 8H, 2 × (C***H***$_2$)$_2$CH$_3$), 0.90 (t, 6H, 2 × C***H***$_3$). MS (ESI) *m*/*z* calcd for ($C_{30}H_{36}N2Se_2$): 584.12. Found: 583.98.

Synthesis of NaRu(4,4′-bis(5-hexylselenophen-2-yl)-2,2′-bipyridine)(4-carboxylic acid-4′-carboxylate-2,2′-bipyridine)(NCS)$_2$ (5, C105). Dichloro(*p*-cymene)ruthenium(II) dimer (0.1051 g, 0.1716 mmol) and **4** (0.2 g, 0.3433 mmol) were dissolved in DMF (50 mL). The reaction mixture was stirred at 80 °C for 4 h under Ar in the dark. Subsequently, 4,4′-dicarboxylic acid-2,2′-bipyridine (0.0838 g, 0.3433 mmol) was added into the flask, and the reaction mixture was stirred at 140 °C for 4 h. At last, an excess of NH_4NCS (1.0450 g, 13.728 mmol) was added to the resulting dark solution, and the reaction continued for another 4 h at the same temperature. Then, the reaction mixture was cooled down to room temperature, and the solvent was removed on a rotary evaporator under a vacuum. Water was added to get a suspended solution. The solid was collected on a sintered glass crucible by suction filtration, washed with water and ether, and dried under a vacuum. The crude complex was dissolved in basic methanol (NaOH) and purified on a Sephadex LH-20 column with methanol as the eluent. The collected main band was concentrated and slowly titrated with an acidic methanol solution (HNO_3) to pH 5.6 monitored by a pH meter. Note that this titration should be done very slowly. When the pH was close to 6.0, the dye molecules were thought to take protons like a buffer reagent. The precipitate was collected on a sintered glass crucible by suction filtration and dried in the air. Yield with four times column purification: 63%. ^{1}H NMR (400 MHz, CD_3OD + NaOD, δ_H): 9.67 (d, 1H), 9.20 (d, 1H), 9.07 (s, 1H), 8.89 (s, 1H), 8.49 (s, 1H), 8.36 (d, 1H), 8.33 (s, 1H), 8.25 (d, 1H), 8.08 (d, 1H), 7.73 (d, 1H), 7.61 (d, 1H), 7.55 (d, 1H), 7.33 (d, 1H), 7.22 (d, 2H), 6.92 (d, 1H), 3.13 (t, 2H, C***H***$_2$(CH$_2$)$_4$CH$_3$), 3.03 (t, 2H, C***H***$_2$(CH$_2$)$_4$CH$_3$), 1.91 (m, 2H, C***H***$_2$(CH$_2$)$_3$CH$_3$), 1.81 (m, 2H, C***H***$_2$(CH$_2$)$_3$CH$_3$), 1.58−1.40 (m, 12H, 2 × (C***H***$_2$)$_3$CH$_3$), 1.03 (t, 3H, C***H***$_3$), 0.98 (t, 3H, C***H***$_3$). Anal. calcd for $NaRuC_{44}H_{43}N_6O_4S_2Se_2 \cdot 2H_2O$: C, 47.96; H, 4.30; N, 7.63%. Found: C, 47.85; H, 4.27; N, 7.67%. MS (ESI) *m*/*z* calcd for ($RuC_{44}H_{43}N_6O_4S_2Se_2$): 1043.02. Found: 1042.58.

UV−Vis, Photoluminescence, and Voltammetric Measurements. Electronic absorption spectra were performed on a UNICO WFZ UV-2802PC/PCS spectrometer. Emission spectra were recorded with a PerkinElmer LS55 luminescence spectrometer. The emitted light was detected with a Hamamatsu R928 red-sensitive photomultiplier. A computer-controlled CHI660C electrochemical workstation was used for square-wave voltammetric measurements in combination with a three-electrode electrochemical cell.

Device Fabrication. A screen-printed single- or double-layer film of interconnected TiO_2 particles was used as a mesoporous negative electrode. The 20-nm-sized TiO_2 particles were first printed on the fluorine-doped SnO_2 (FTO) conducting glass electrode and further coated by a 5-μm-thick second layer of 400-nm-sized light-scattering anatase particles if it was needed. The film thickness was measured using a benchtop Ambios XP-1 stylus profilometer. The detailed preparation procedures of TiO_2 nanocrystals, pastes for screen-printing, and the nanostructured TiO_2 film have been reported in a previous paper.[12] A cycloidal TiO_2 electrode (~0.28 cm^2) was stained by immersing it into a dye solution containing C105 sensitizer (300 μM) and cheno (300 μM) in a mixture of acetonitrile and *tert*-butanol (volume ratio: 1:1) overnight. After washing with acetonitrile and drying by air flow, the sensitized titania electrode was assembled with a thermally platinized FTO electrode. The electrodes were separated by a 30-μm-thick Bynel (DuPont) hot-melt gasket and sealed up by heating. The internal space was filled with a liquid electrolyte using a vacuum back-filling system. The electrolyte-injecting hole on the counterelectrode glass substrate, made with a sand-blasting drill, was sealed with a Bynel sheet and a thin glass cover by heating.

Photovoltaic Characterization. A LS100 solar simulator (Solar Light Com. Inc., USA) was used to give an irradiance of 100 mW cm^{-2} (the equivalent of one sun at AM1.5G) at the surface of a testing cell. The current−voltage characteristics of the cell under these conditions were obtained by applying external potential bias to the cell and measuring the generated photocurrent with a Keithley model 2400 digital source meter. This process was fully automated using Labview 8.0. A similar data acquisition system was used to control the incident photon-to-collected electron conversion efficiency (IPCE) measurement. Under full computer control, light from a 1000 W xenon lamp was focused through a monochromator onto the photovoltaic cell being tested. A computer-controlled monochromator (Omni λ300) was incremented through the spectral range 300−900 nm to generate photocurrent action spectra with a sampling interval of 10 nm and a current sampling time of 2 s. IPCE is defined by IPCE(λ) = $hcJ_{sc}/e\phi\lambda$, where h is the Planck constant, c is the light speed in vacuum, e is the electronic charge, λ is the wavelength (m), J_{sc} is the short-circuit photocurrent density (A m^{-2}), and ϕ is the incident radiative flux (W m^{-2}). Photovoltaic performance was measured by using a metal mask with an aperture area of 0.158 cm^2.

Results and Discussion

In dye-sensitized solar cells, titania does not make a large contribution to light-harvesting due to a wide bandgap as well as a relatively small portion of ultraviolet photons in the AM1.5G solar spectrum.[13] Also, direct-band excitation of mesoporous titania will create highly oxidative holes in its deep valence band or hole trapping states at energy levels close to its valence band.[14] These holes not only decompose the organic materials such as dyes and electrolytes in view of the long-term device operation but also drive down the quasi-Fermi level of sensitized titania, reducing the open-circuit photovoltage (V_{oc}) and power conversion efficiency

(12) Wang, P.; Zakeeruddin, S. M.; Comte, P.; Charvet, R.; Humphry-Baker, R.; Grätzel, M. *J. Phys. Chem. B* **2003**, *107*, 14336.
(13) Hagfeldf, A.; Grätzel, M. *Chem. Rev.* **1995**, *95*, 49.
(14) Legrini, O.; Oliveros, E.; Braun, A. M. *Chem. Rev.* **1993**, *93*, 671.

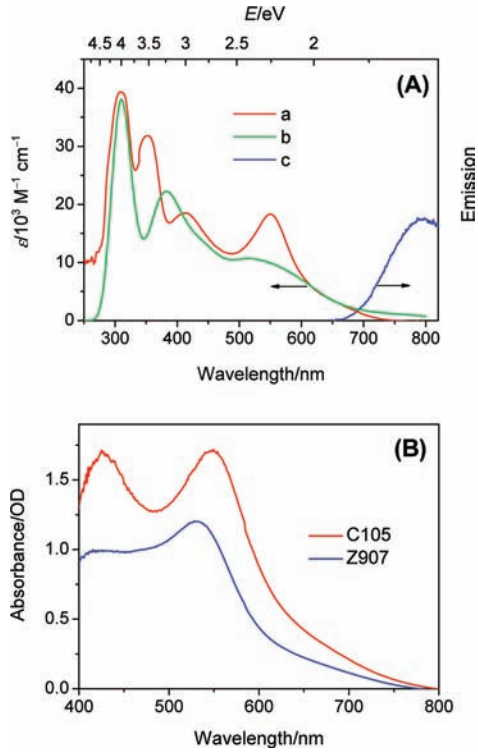

Figure 1. (A) Experimental (a) and calculated (b) electronic absorption spectra and (c) emission spectrum of C105 sensitizer in DMF. (B) Absorption spectra of C105 and Z907 anchored on a 7.5-μm-thick mesoporous titania film.

slightly. Fortunately, the ultraviolet photons will be filtered off by the employed antireflection coating film with a function to enhance the light absorption in the visible region. On the other hand, electrolytes or hole transporting materials do not contribute to the sensitization of wide bandgap titania. Thereby, the sensitizer is the only element in practical DSCs used to capture photons, and its spectral overlapping with the AM1.5G solar irradiance spectrum is the first factor determining the photocurrent and cell efficiency. Thus, we measured the light absorption of our C105 dye both in the solution and, more importantly, anchored on the mesoporous titania film.

As presented in Figure 1A, the electronic absorption spectrum of the C105 dye has two intense absorption bands at 309 and 353 nm in the UV region and the characteristic metal-to-ligand charge-transfer transition (MLCT) absorption bands in the visible region like other heteroleptic polypyridyl ruthenium(II) complexes.[6] In DMF, the low-energy MLCT transition absorption peaks at 550 nm, which is 27 nm red-shifted compared to that of Z907 or its analogues.[15] The measured molar extinction coefficient (ε) at 550 nm is 18.4 $\times$ 10^3 M^{-1} cm^{-1}, which is remarkably higher than the corresponding values for the standard Z907 (12.2 $\times$ 10^3 M^{-1} cm^{-1}) and N719 (14.0 $\times$ 10^3 M^{-1} cm^{-1}) sensitizers.[15] In comparison to its analogue C102 or C101 with furan or thiophene conjugation,[3c] the C105 dye with selenophene shows an improved absorption cross-section. It is also noted that the molar extinction coefficient increases in the order of C105 > C101 > C102 (17.5 $\times$ 10^3 M^{-1} cm^{-1} at 547 nm for C101; 16.8 $\times$ 10^3 M^{-1} cm^{-1} at 547 nm for C102),[3c] consistent with the electropositivity trend and the size of the heteroatoms (Se > S>O) of five-member conjugated units. The calculated optical spectrum shown in Figure 1A is in close agreement with the experimental data, ensuring the correct assignments of different electronic transitions. Transition-involved molecular orbitals are shown in Figure S1 and detailed transition assignments are summarized in Table S1 of the Supporting Information. Obviously, we can see that, induced by the absorption of visible photons, the electrons delocalized over ruthenium and NCS are excited to final electronic states that mainly dispersed on the bipyridyl ligands. The transition led to a hole dispersed over NCS with a sizable population on the far end sulfur atom, giving spatial convenience for dye regeneration. Note that the transition from the highest occupied orbital (HOMO) to the ancillary ligand also makes a large contribution to the low-energy MLCT transition shown in Figure 1A, resulting in an enhanced absorption coefficient, due to an augmented oscillator strength in the case of selenium heteroatoms. Furthermore, our calculation (Figure S2, Supporting Information) has also proved that the lowest unoccupied orbital (LUMO) energy of the spectator ligand aligns in the order of O > S > Se, which may explain the slightly red-shifted MLCT absorption of C105 relative to C102 and C101. As shown in Figure 1A, excitation of the low-energy MLCT transitions of the C105 sensitizer in DMF produces a triplet emission centered at 800 nm.

It is noted that, apart from the molar extinction coefficient, the molecular diameter and packing mode also have a strong influence on the optical absorptivity of stained mesoporous films; thus, we further measured the film absorption closely related to the light-harvesting of dye-sensitized solar cells. The impressive improvements of extending the π-conjugated system of ancillary ligands in heteroleptic ruthenium complexes are evident in Figure 1B, which depicts the absorption spectra in the visible region of Z907 and C105 anchored on a 7.5-μm-thick transparent nanocrystalline TiO_2 film. Note that absorbance at different wavelengths of stained films increases linearly along with the film thickness. The C105 sensitizer confers an improved light absorption to the stained mesoporous TiO_2 film, which is highly desirable, as it allows using thinner nanocrystalline layers to sustain good light-harvesting, facilitating charge collection in practical DSCs. Decreasing the film thickness also augments the open-circuit photovoltage of the cell due to the reduced reverse saturation current and the increase of electron density, lifting up the electron quasi-Fermi level of titania.

Having good light absorption in a dye does not guarantee it for high-efficiency dye-sensitized solar cells. A critical step in the operation of solar cells is the charge separation of the excited electron−hole pair (exciton) created upon photon absorption.[16] This charge separation is triggered at the interface between a donor component and an acceptor

(15) (a) Zakeeruddin, S. M.; Nazeeruddin, M. K.; Humphry-Baker, R.; Péchy, P.; Quagliotto, P.; Barolo, C.; Viscard, G.; Grätzel, M. *Langmuir* **2002**, *18*, 952. (b) Wang, P.; Wenger, B.; Humphry-Baker, R.; Moser, J.-E.; Teuscher, J.; Kantlehner, W.; Mezger, J.; Stoyanov, E. V.; Zakeerddin, S. M.; Grätzel, M. *J. Am. Chem. Soc.* **2005**, *127*, 6850.

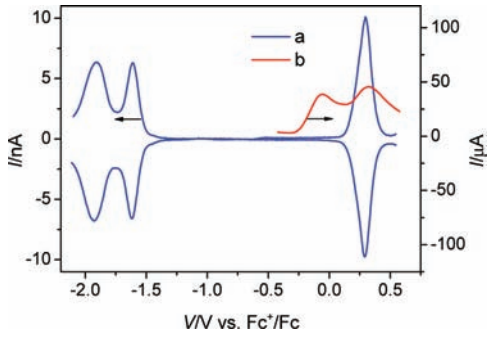

Figure 2. Square-wave voltammogram of a Pt ultra-microelectrode in a DMF solution containing the C105 dye (a) and 0.1 M tetra-*n*-butylammonium hexafluorophosphate as the supporting electrolyte. The square-wave voltammogram of 1-ethyl-3-methylimidazolium iodide (b) in acetonitrile with 0.1 M 1-ethyl-3-methylimidazolium bis(trifluorosulfonyl)imide as the supporting electrolyte was recorded with a thermally platinized FTO electrolyte. The LUMO and HOMO were estimated vs a vacuum: $E_{LUMO/HOMO} = -4.88 - F\phi_{redox}$.

component (dye and tiatnia in DSCs) with a thermodynamical energy offset. Here, we used the ultra-microelectrode square-wave voltammetry technique to measure the HOMO and LUMO of the C105 dye in a nitrogen-filled glovebox. As shown in Figure 2, the downhill energy offset by the measured LUMO (−3.37 eV vs vacuum) of the C105 dye relative to the conduction band edge[2b,13] (−4.00 eV vs vacuum) of TiO_2 provides the driving force for charge generation. Furthermore, photoinjected electrons in the titania need to be diffused through a several micrometer-thick film to the current collector within the millisecond time domain; however, in the absence of electrolytes, the oxidized sensitizer can recapture electrons within the submillisecond time domain.[2c] Due to the inconsistency of the iodide redox potentials mentioned in the literature,[13,17,18] we measured it in the exact solvent of acetonitrile often used for DSCs. Owing to the sluggish electron transfer kinetics of iodide on the normal Pt or FTO electrode, we coated a FTO electrode using the thermal platinization method to considerably reduce the oxidation overpotential and measured its redox potential and HOMO accurately. The measured redox potential of iodide is about −0.06 V versus Fc^+/Fc. The uphill energy offset by the HOMO of C105 (−5.05 eV vs vacuum) in contrast to that (−4.64 eV) of iodide could lead to fast dye regeneration, avoiding the geminate charge recombination between oxidized dye molecules and photoinjected electrons in the nanocrystalline titania film.

In order to fairly evaluate the photovoltaic performance of this new sensitizer, we compared it with the standard Z907 amphiphilic dye using mesoporous titania films with different thicknesses. Figure 3A and B present the typical photocurrent action spectra of cells with the corresponding C105 and Z907 sensitizers. We have found that, if the cells employ a thin transparent titania film, photocurrent action spectra (curves a in Figure 3A and B) closely follow the absorption spectra (Figure 1B) of mesoporous titania films stained with the

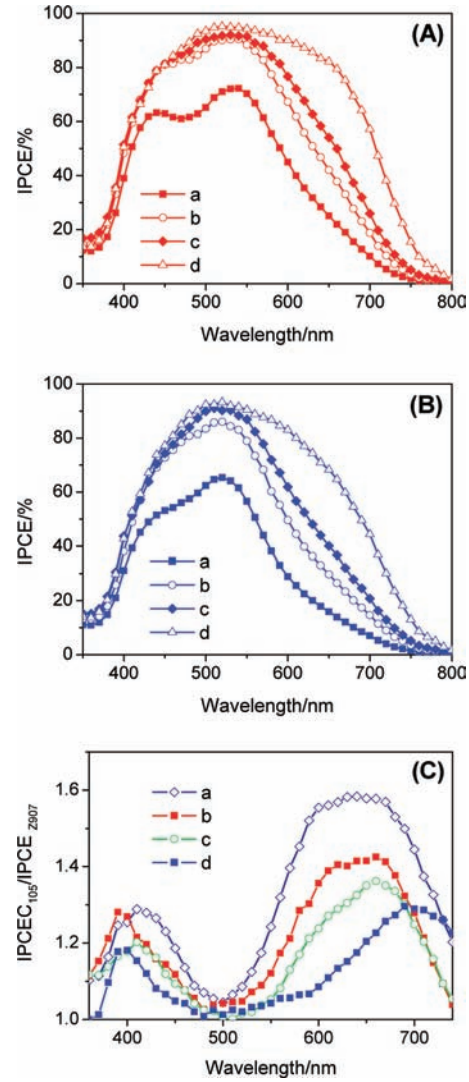

Figure 3. (A) Photocurrent action spectra of cells with the C105 dye. (B) Photocurrent action spectra of cells with the Z907 dye. (C) The ratio of monochromatic incident photon-to-collected electron conversion efficiency: (a) 2.7 μm mesoporous titania film, (b) 5.2 μm mesoporous titania film, (c) 7.5 μm mesoporous titania film, and (d) double-layer film with 9 μm mesoporous titania and 5 μm scattering layer. An antireflection film was adhered to cells during measurements.

C105 and Z907 dyes, apart from a small distortion in the blue region due to the dissipative absorption of triiodide in the electrolyte. Along with the increase in film thickness and especially the usage of a light-scattering scattering layer, photocurrent action spectra in the red region have been significantly enhanced and do not look like the absorption spectra, owing to the saturated absorption in the green region. A close look at the ratio of IPCEs (Figure 3C) of the C105 and Z907 dyes has evidently revealed the merit of enhancing optical absorptivity of stained titania films with high molar extinction coefficient sensitizers, especially in the weak absorption red region as well as the blue region, where competitive triiodide absorption is wasteful. Detailed cell parameters based on different titania films are summarized in Table 1, showing that the C105 dye is more efficient than Z907.

We further formulated a new electrolyte composed of 1.0 M DMII, 50 mM LiI, 30 mM I_2, 0.5 M *tert*-butylpyridine,

(16) Brédas, J.-L.; Beljonne, D.; Coropceanu, V.; Cornil, J. *Chem. Rev.* **2004**, *104*, 4971.
(17) Peter, L. M. *J. Phys. Chem. C* **2007**, *111*, 6601.
(18) Bard, A. J.; Faulkner, L. R. *Electrochemical Methods: Fundamentals and Applications*, 2nd ed.; Wiley: Weinheim, Germany, 2001.

Table 1. Detailed Photovoltaic Parameters of Cells Made with the C105 and Z907 Sensitizers Employing Different Films[a]

thickness/μm	dye	J_{sc}/mA cm^{-2}	V_{oc}/mV	FF	η/%
2.7	C105	10.11	780.4	0.732	5.78
	Z907	8.57	796.3	0.707	4.83
5.4	C105	13.29	759.0	0.734	7.41
	Z907	11.98	763.8	0.714	6.53
7.5	C105	15.10	749.5	0.739	8.37
	Z907	13.65	766.3	0.720	7.54
double layer	C105	18.09	747.8	0.744	10.06
9 + 5	Z907	16.37	767.2	0.717	9.00

[a] The electrolyte composition is as follows: 1.0 M DMII, 50 mM LiI, 30 mM I_2, 0.5 M *tert*-butylpyridine, and 0.1 M GNCS in the mixed solvent of acetonitrile and valeronitrile (v/v, 85:15).

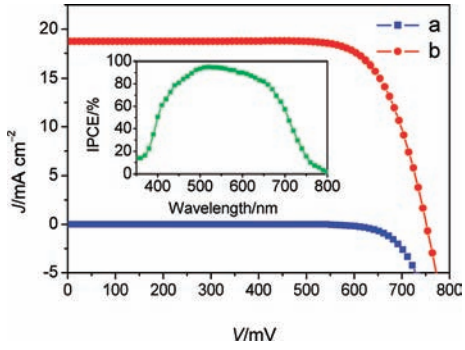

Figure 4. $J-V$ characteristics of a high-efficiency DSC with the C105 sensitizer measured (a) in the dark and (b) under the illumination of AM1.5G sunlight (100 mW cm^{-2}). Aperture area of the testing mask: 0.158 cm^2. The inset is its photocurrent action spectrum. Film thickness: 10 + 5. An antireflection film was adhered to the cell during measurements. The electrolyte composition is as follows: 1.0 M DMII, 50 mM LiI, 30 mM I_2, 0.5 M *tert*-butylpyridine, and 0.1 M GNCS in acetonitrile.

and 0.1 M GNCS in acetonitrile rather than the mixed solvents of acetonitrile and valeronitrile, to make a more efficient cell along with a 10 + 5 film. We have found that different dyes need compatible solvents for their electrolytes to obtain a high efficiency. A systematic comparison on this topic will be separately published. As shown in Figure 4, this cell has a short-circuit photocurrent density (J_{sc}) of 18.74 mA cm^{-2}, an open-circuit photovoltage (V_{oc}) of 754 mV, and a fill factor (FF) of 0.751, yielding an overall conversion efficiency (η) of 10.61%. At various lower incident light intensities, overall power conversion efficiencies are even higher, up to 10.8%. Under the similar conditions, a reference cell with C101 dye exhibits 11% efficiency.[3c] We note that the present challenge of this C105 dye lies in a relatively lower photovoltage and a lower fill factor in contrast to C101. The exact origins and solutions need to be addressed in our further work. The photocurrent action spectrum of a high-efficiency DSC with the C105 sensitizer is shown in the inset of Figure 4. The IPCEs exceed 60% in the whole visible spectral region, with a broad plateau of over 80% from 450 to 650 nm, reaching a maximum of 95% at 520 nm. Considering the light absorption and scattering loss of the conducting glass, the maximum efficiency for absorbed photon-to-collected electron conversion efficiency is close to unity over a broad spectral range. From the overlap integral of this curve with the standard AM1.5G solar emission spectrum, a short-circuit photocurrent density (J_{sc}) of 18.75 mA cm^{-2} is calculated, which is in excellent agreement with the measured photocurrent density. Therefore, there is a negligible spectral mismatch between our solar simulator and the standard AM1.5G sunlight. In addition, our preliminary tests with a solvent-free ionic liquid electrolyte containing *N*-butylbenzimidazole have shown that this new sensitizer is very stable under prolonged thermal and light-soaking stress, proving the success of introducing selenophene units into sensitizers for DSCs.

Conclusion

In summary, we have developed a high molar extinction coefficient ruthenium sensitizer featuring an electron-rich selenophene unit, to considerably enhance the optical absorptivity of mesoporous titania films. The increase of the molar extinction coefficient of heteroleptic ruthenium dyes (C105 > C101 > C102) follows the electropositivity tendency and the size of the heteroatoms (Se > S > O) of electron-rich units in conjugation with bipyridine. For a newly developed dye, the achievement of over 10.6% power conversion efficiencies is very encouraging. We are now systematically optimizing the cell parameters to explore the full potential of this promising sensitizer.

Acknowledgment. The National Key Scientific Program (No. 2007CB936700), the National Science Foundation of China (No. 50773078), the "CAS 100-Talent Program", and the "CAS Knowledge Innovation Program" have supported this work. We are grateful to Dyesol for supplying 400-nm-sized scattering paste and to DuPont Packaging and Industrial Polymers for supplying the Bynel film.

Supporting Information Available: Calculation details. This material is available free of charge via the Internet at http://pubs.acs.org.

IC802289E